Separation between Low-Energy Hole Dynamics and Spin Dynamics in a Frustrated Magnet

Kou Takubo,[1] Yusuke Nambu,[2] Satoru Nakatsuji,[2] Yuki Wakisaka,[1] Takaaki Sudayama,[1] David Fournier,[3] Giorgio Levy,[3] Andrea Damascelli,[3] Masashi Arita,[4] Hirofumi Namatame,[4] Masaki Taniguchi,[4,5] and Takashi Mizokawa[1,4]

[1]*Department of Physics & Department of Complexity Science and Engineering, University of Tokyo, 5-1-5 Kashiwanoha, Chiba 277-8561, Japan*

[2]*Institute for Solid State Physics, University of Tokyo, Kashiwa, Chiba 277-8581, Japan*

[3]*Department of Physics and Astronomy, University of British Columbia, Vancouver, B.C., V6T 1Z4, Canada*

[4]*Hiroshima Synchrotron Radiation Center, Hiroshima University, Higashihiroshima, Hiroshima 739-0046, Japan*

[5]*Graduate School of Science, Hiroshima University, Higashihiroshima, Hiroshima 739-8526, Japan*

(Received 7 August 2009; published 3 June 2010)

An angle-resolved photoemission spectroscopy (ARPES) study is reported on a Mott insulator $NiGa_2S_4$ in which Ni^{2+} ($S = 1$) ions form a triangular lattice and the Ni spins do not order even in its ground state. The first ARPES study on the two-dimensional spin-disordered system shows that low-energy hole dynamics at high temperatures is characterized by wave vectors Q_E which are different from wave vectors Q_M dominating low-energy spin excitations at low temperatures. The unexpected difference between Q_E and Q_M is deeply related to charge fluctuation across the Mott gap in the frustrated lattice and is a key issue to understand the spin-disordered ground states in Mott insulators.

DOI: 10.1103/PhysRevLett.104.226404 PACS numbers: 71.10.Pm, 75.40.−s, 79.60.−i

Since Anderson proposed the possibility of a resonating valence bond state in frustrated magnets [1], exotic ground states without conventional spin order have been discovered in various organic and inorganic Mott insulators on frustrated lattices [2–6]. Magnetic properties of Mott insulators are primarily described by models made up from localized spins, and the charge excitation across the Mott gap has a secondary role to give the exchange interaction J between the localized spins. The exchange interaction J in a Mott insulator is roughly given by $-2t^2/U$, where t is the transfer integral between the two localized orbitals and U is the charge excitation energy across the Mott gap. Near the Mott transition, the Mott insulator has small U and, consequently, has large J. Therefore, it is natural that nonfrustrated Mott insulators with small U tend to have conventional spin orders. This situation is dramatically changed in Mott insulators on geometrically frustrated lattices. Theoretical studies on triangular-lattice Hubbard models have shown that a spin-disordered phase may be realized near the Mott transition [7–9]. Actually, the spin-disordered Mott insulators ever found all have relatively small Mott gap [2–6], suggesting that the charge fluctuation across the Mott gap on the geometrically frustrated lattices would be important to realize the spin-disordered ground states.

The interplay between the charge fluctuation and the spin dynamics near the Mott transition manifests in dynamics of electron or hole created in the spin-disordered states. Normally, Mott insulators with conventional spin orders are known to have low-energy electron or hole dynamics governed by their dominant spin correlation. On the other hand, frustrated Mott insulators without conventional spin orders may exhibit a fundamentally new electron or hole dynamics such as spin-charge separation [10,11], owing to quantum effects due to highly degenerate states close to quantum criticality. Spin-disordered Mott insulators may have hidden orders such as spin nematic order [12–15], vortex-induced topological order [16], and scalar or vector chiral orders [17,18] which are currently attracting intensive research activities in the context of topological transition, multiferroics, spintronics, etc. It is expected that the effects of such hidden orders manifest in the electron or hole dynamics. In this context, it is highly desirable to study the hole dynamics of frustrated Mott insulators using angle-resolved photoemission spectroscopy (ARPES).

Among the frustrated Mott insulators, $NiGa_2S_4$ has a frustrated Ni^{2+} ($S = 1$) triangular lattice and shows a spin-disordered ground state [3]. The magnetic part of the specific heat at low temperature has T^2 dependence and does not depend on applied magnetic field, indicating two-dimensional gapless spin excitations on the triangular lattice. The magnetic neutron scattering of $NiGa_2S_4$ exhibits a broad structure at $Q_M = 0.57$ Å^{-1} below 10 K that is associated with the incommensurate short-range spin correlation. Theoretical studies suggested that the unusual magnetic properties of $NiGa_2S_4$ can be described by spin models with higher order exchange terms [12–16], indicating that the proximity to the Mott transition is important. Since single crystals with charge neutral cleavage planes or van der Waals gaps [Fig. 1(a)] are successfully synthesized only in $NiGa_2S_4$ among the spin-disordered Mott insulators [3], $NiGa_2S_4$ is an ideal material for ARPES. In the present Letter, we report on an ARPES study of $NiGa_2S_4$. The ARPES results show that $NiGa_2S_4$ has the low-energy hole dynamics characterized by wave vectors Q_E which are

 © 2010 The American Physical Society

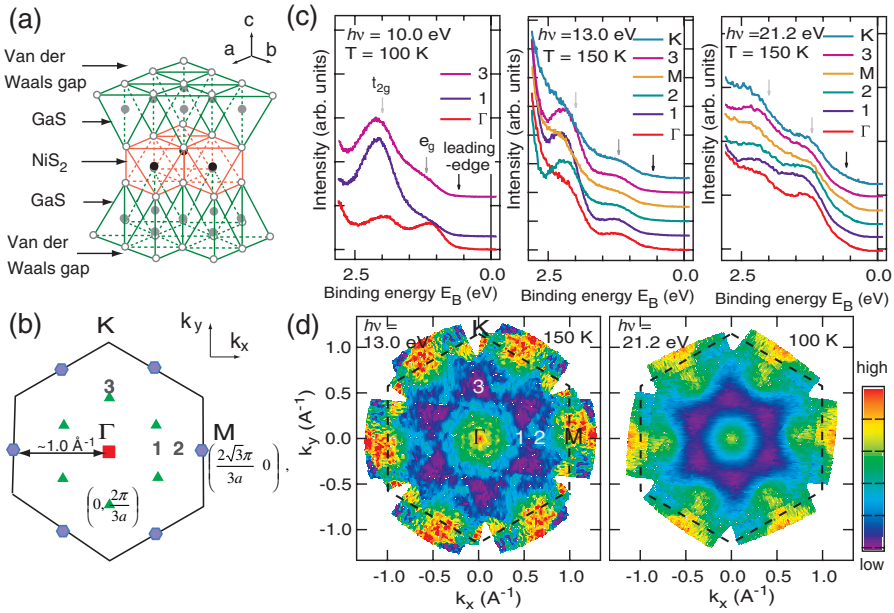

FIG. 1 (color online). (a) A schematic drawing of the NiS_2 and GaS layers in $NiGa_2S_4$. The black, closed gray and open gray circles represent Ni, Ga, and sulfer ions, respectively. (b) The triangular-lattice Brillouin zone of the NiS_2 layer. The solid hexagons and square indicate the wave vectors for the bottoms of the doublon and holon excitations, respectively, that are obtained for the half-filled triangular lattice in Ref. [23]. The doublon minimum points are located at the M points of $(\pm 2\sqrt{3}\pi/3a, 0)$ and $(\pm\sqrt{3}\pi/3a, \pm\pi/a)$, and the holon minimum point is located at the origin. The spinon minimum points (triangles) are located around $k = (0, \pm 2\pi/3a)$ and $(\pm\sqrt{3}\pi/3a, \pm\pi/3a)$ as obtained by the neutron scattering experiments at low temperature [3]. (c) Overall valence-band spectra of $NiGa_2S_4$ taken at different photon energies of $h\nu = 10.0$ (left), 13.0 (middle), and 21.2 eV (right). The spectra labeled as 1, 2, and 3 are taken at 1/2 and 3/4 of the Γ-M cut and at 1/2 of the Γ-K cut in the Brillouin zone, respectively. (d) Intensity mappings of ARPES ($h\nu = 13.0$ and 21.2 eV) at $E_B = 0.6$ eV. The energy windows are fixed to 0.05 eV. Dashed lines indicate the Brillouin zone of the triangular lattice.

different from wave vectors Q_M dominating low-energy spin excitations at low temperatures. The unexpected separation between Q_E and Q_M is deeply related to unusual quantum critical behaviors in frustrated magnets near Mott transition and is a key issue to understand natures of spin-disordered ground states.

Single crystals of $NiGa_2S_4$ were grown by chemical vapor transport as described previously [19]. ARPES measurements on $NiGa_2S_4$ were performed at Quantum Materials Laboratory, University of British Columbia (UBC) using SPECS 2D-Phoibos150 analyzer equipped with a monochromatized He I discharge lamp ($h\nu =$ 21.2 eV), and at beam line 9 A, Hiroshima Synchrotron Radiation Center (HSRC) using a SCIENTA R4000 analyzer with photon energy $h\nu = 10.0$, 13.0, and 23.0 eV. In the ARPES measurements at UBC, the total energy resolution was set to ~40 meV and the angular resolution was ~0.3°. The linear polarization of the incident beam was 45° off the sample surface. The base pressure of the spectrometer was 1×10^{-8} Pa. In the ARPES measurements at HSRC, the total energy resolution was set to ~30 meV at 13.0 eV. The angular resolution was 0.3°. The circular polarization of the incident beam is 45° off the sample surface. The base pressure was 1×10^{-8} Pa. The single crystals were cleaved *in situ* in order to obtain clean surfaces. The cleaved surfaces were the *ab* planes and the NiS_2 triangular lattices were parallel to the cleaved surface [Fig. 1(a)]. All photoemission data were collected within 12 hours after cleaving. As expected from the layered structure of $NiGa_2S_4$, the obtained surfaces were clean and stable. The results were robust from cleave to cleave. All ARPES data were measured in the temperature range between 100 and 200 K and did not show clear temperature dependence. At low temperatures below ~80 K, the samples were charged up preventing ARPES measurement.

The hexagonal Brillouin zone (BZ) of $NiGa_2S_4$ is shown in Fig. 1(b). Overall ARPES spectra taken at selected momentum points of the BZ with $h\nu = 10.0$, 13.0, and 21.2 eV are displayed in Fig. 1(c). The spectral feature at ~0.6 eV is the leading edge of the valence-band with the Ni 3d e_g character. The main Ni 3d e_g band and the Ni 3d t_{2g} band are located at ~1.2 and 2.0 eV, respectively. Figure 1(d) shows ARPES intensity mappings at 0.6 eV as functions of wave vectors. In order to show the mapping for the entire BZ, the intensity mappings are symmetrized considering the sixfold rotational symmetry of $NiGa_2S_4$. The leading edges or the maximum points of the e_g band are located around $k = (\pm 2\sqrt{3}\pi/3a, 0)$ and $(\pm\sqrt{3}\pi/3a, \pm\pi/a)$, the M points of the BZ, as well as the region around the Γ point. Interestingly, the wave vectors between the two maximum points are $Q_E = (\pm 2\sqrt{3}\pi/3a, 0)$ and

$(\pm\sqrt{3}\pi/3a,\ \pm\pi/a)$ which are different from the peak positions Q_M [$\sim (\pm\sqrt{3}\pi/3a, \pm\pi/3a)$ and $(0, \pm 2\pi/3a)$] in the neutron scattering data [3]. This observation in $NiGa_2S_4$ is in sharp contrast to the parent materials of cuprate superconductors which are nonfrustrated Mott insulators. In the cuprates, the leading edges or the maximum points are located at $k = (\pm\pi/2a, \pm\pi/2a)$, and the wave vectors $Q = (\pm\pi/a, \pm\pi/a)$ between the two maximum points correspond to the periodicity of spin ordering [20].

This observation shows that the topmost Ni $3d$ e_g band has a peculiar band folding related to spin or charge correlations with Q_E while a very flat Ni $3d$ e_g band along the Γ-M direction is expected from the band calculations using both of a local-density-approximation calculation [21] and a model Hartree-Fock (HF) calculation [22]. In order to see detailed dispersions of the Ni $3d$ e_g band, intensity plots along Γ-M and Γ-K directions are displayed in Figs. 2(a) and 2(b), respectively. While the energy distribution curves are rather broad as shown in Figs. 2(c) and 2(d), the distinct dispersions are observed on the ARPES data along the Γ-M and Γ-K directions. The band dispersion along Γ-M takes its maximum around $k = 0$ and $k = 1.0$ Å^{-1} ($\sim 1.15\pi/a$ or $\pm 2\sqrt{3}\pi/3a$) consistent with the band folding in Fig. 1(d). The similar dispersion is also observed along Γ-K because the maximum region centered at the M point is extended to the K point as seen in Fig. 1(d). This indicates that, although the instability with Q_E is dominant, the instability with Q'_E is almost degenerate with the primary instability with Q_E as illustrated in Fig. 3(a). The band folding may originate from the short-range magnetic correlation with Q_M that develops at low temperatures [3]. However, the wave vectors Q_E (Q'_E) between the maximum regions at the Γ point and at the M (K) point are different from Q_M. Therefore, the wave vector Q_E and Q'_E should be attributed to other spin or charge correlations at high temperatures.

The spin-disordered system can be characterized by the gapless spin channel and the gapped charge channel. One natural mechanism to lead the separation between Q_M and Q_E seen above would be spin-charge separation. If one assumes spin-charge separation in the spin-disordered system, the gapless spin and gapped charge excitations are described by spinons and holons or doublons, respectively [23]. The spinon excitation takes its minimum at $Q_M \sim (0, \pm 2\pi/3a)$ and $(\pm\sqrt{3}\pi/3a, \pm\pi/3a)$ seen in the neutron scattering experiments, and the holon excitation is expected to take its minimum at the Γ point [See also Fig. 1(b)]. Since the ARPES data are taken at 100 and 150 K that are higher than the Weiss temperature $T_{\mathrm{Weiss}} \sim 80$ K, the momentum distribution of spinons can be neglected and the leading edge of ARPES spectrum should be located at the Γ point. However, in the present ARPES result, the leading edge is also located at the M point which is close to the minimum of doublon excitation. Therefore, in the spin-charge separation picture, the present ARPES result indicates that the holon and doublon excitations are mixed or the holon and doublon form a kind of exciton to give charge modulation with Q_E [see Fig. 3(b)] as proposed on a spin-disordered triangular lattice near the quantum critical point of the Mott transition [23].

Instead of the spin-charge separation scenario, one may consider excitons formed between holes in the lower

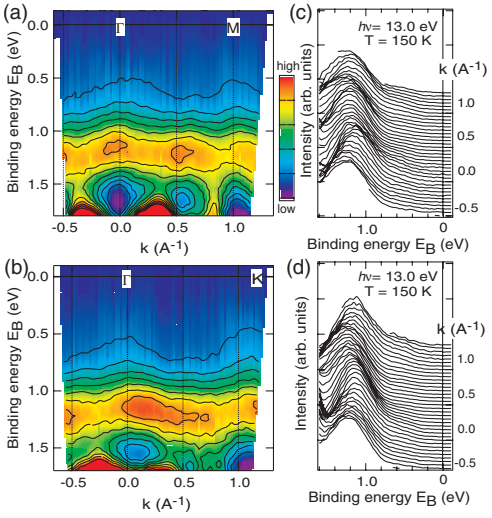

FIG. 2 (color online). Intensity plots for the Ni $3d$ e_g band along the (a) Γ-M and (b) Γ-K directions. The Ni $3d$ e_g contribution is obtained by subtracting the Ni $3d$ t_{2g} contribution from the ARPES data. The solid curves are the contours. (c) and (d) are the energy distribution curves for (a) and (b), respectively.

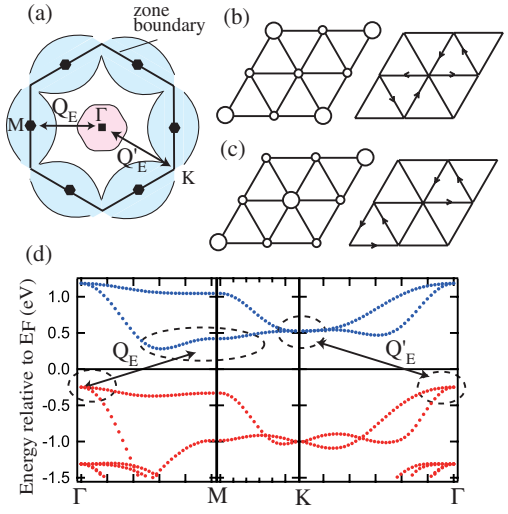

FIG. 3 (color online). (a) Schematic picture for the leading edge region observed in ARPES. (b) Charge order model and current model consistent with the band folding with Q_E. The size of open circles indicates the charge modulation. The arrows indicate the current directions. (c) Charge order model and current model consistent with the band folding with Q'_E. (d) Excitonic coupling with Q_E or Q'_E between the upper and lower Hubbard bands. The upper and lower Hubbard bands are shown by the dots which are calculated by unrestricted Hartree-Fock approximation [22].

Hubbard band $v_{k,\sigma}$ and electrons in the upper Hubbard band $c_{k,\sigma}$ of the small U Mott insulators [24,25] as illustrated in Fig. 3(d). Here, k and σ represent the wave vector and spin of electrons, respectively. The formation of such excitons with real $\langle \sum_k v^+_{k,\sigma} c_{k+Q_E,-\sigma} \rangle$ corresponds to charge ordering shown in Fig. 3(b) and leads to the band folding with Q_E. On the other hand, imaginary $\langle \sum_k v^+_{k,\sigma} c_{k+Q_E,-\sigma} \rangle$ ($\langle \sum_k v^+_{k,\sigma} c_{k+Q_E,\sigma} \rangle$) corresponds to orbital current order (spin current order) which is shown in Fig. 3(b) and provides the band folding with Q_E [25].

When the Hubbard model for $NiGa_2S_4$ is mapped onto a spin model, one can consider effects of biquadratic exchange terms of $K(S_iS_j)^2$ which provide quadrupole-quadrupole interaction between the ith and jth Ni sites [10,12,14–16]. When U is small enough, the biquadratic exchange terms can be large compared to Heisenberg exchange terms JS_iS_j and can induce a spin nematic order with Q_E, which is consistent with the ARPES result. Another possibility is that current states with scalar or vector spin chiral order of Q_E are stabilized by the ring exchange term $K(S_iS_j)(S_kS_l)$ which can be enhanced in the small U Mott insulators [17]. Such orbital or spin current states may correspond to the excitonic insulator states with imaginary order parameters.

The present ARPES result indicates that the spin nematic correlation or the spin chiral correlation with Q_E would exist at high temperatures and that $NiGa_2S_4$ is close to a quantum critical point between the spin dipole order and the spin nematic order (or the spin chiral order). Interestingly, the observed Q_E is given by $Q_{M1} + Q_{M2}$ where Q_{M1} and Q_{M2} are two of the six wave vectors for Q_M induced by the antiferromagnetic Heisenberg exchange term between the third nearest neighbors. Therefore, the observed correlation with Q_E naturally indicates the importance of the biquadratic or ring exchange interactions mentioned above. Here, it would be interesting to speculate the relationship between the exciton picture and the exchange picture. The spin nematic correlation and spin chiral correlation would be related to a formation of excitons with rotonlike minimum at wave vectors Q_E while the Bose-Einstein condensation of the triplet exciton at wave vector Q_M corresponds to the spin dipole order.

In the spin-disordered material $NiGa_2S_4$, the valence band maximum at $k = (0, 0)$ is folded onto the regions at $k = (\pm 2\sqrt{3}\pi/3a, 0)$ and $(\pm\sqrt{3}\pi/3a, \pm\pi/a)$, showing that the hole dynamics is characterized by the wave vectors $Q_E = (\pm 2\sqrt{3}\pi/3a, 0)$ and $(\pm\sqrt{3}\pi/3a, \pm\pi/a)$ which are different from Q_M dominating the spin dynamics at low temperatures. The band folding can be attributed to excitonic correlations between holons and doublons or those between lower-Hubbard-band holes and upper-Hubbard-band electrons near the Mott transition. This result shows that, in a frustrated lattice with small Mott gap, the excitonic instability with Q_E becomes relevant as suggested by Mott [24], and the separation between Q_E and Q_M plays essential roles to prevent long-range spin orders at low temperatures. Within a spin model, the band folding with Q_E can be attributed to spin nematic or spin chiral instability due to the higher order exchange terms enhanced by the proximity to the Mott transition.

We acknowledge valuable discussions with S. Onoda, Y. B. Kim, and D. I. Khomskii. The synchrotron radiation experiments have been done with the approval of HSRC (Proposals No. 06-A-49 and No. 08-A-2). This work is partially supported by Grant-in-Aid (No. 21684019) from the Japanese Society for the Promotion of Science, and also by Grant-in-Aid for Scientific Research on Priority Areas (No. 17071003, 19052003) from the Ministry of Education, Culture, Sports, Science and Technology, Japan.

[1] P. W. Anderson, Mater. Res. Bull. **8**, 153 (1973).
[2] Y. Shimizu *et al.*, Phys. Rev. Lett. **91**, 107001 (2003).
[3] S. Nakatsuji *et al.*, Science **309**, 1697 (2005).
[4] J. S. Helton *et al.*, Phys. Rev. Lett. **98**, 107204 (2007).
[5] Y. Okamoto, M. Nohara, H. Aruga-Katori, and H. Takagi, Phys. Rev. Lett. **99**, 137207 (2007).
[6] S. Yamashita *et al.*, Nature Phys. **4**, 459 (2008).
[7] H. Morita, S. Watanabe, and M. Imada, J. Phys. Soc. Jpn. **71**, 2109 (2002).
[8] O. I. Motrunich, Phys. Rev. B **72**, 045105 (2005).
[9] T. Senthil, Phys. Rev. B **78**, 045109 (2008).
[10] A. Läuchli and D. Poilblanc, Phys. Rev. Lett. **92**, 236404 (2004).
[11] S.-S. Lee and P. A. Lee, Phys. Rev. Lett. **95**, 036403 (2005).
[12] H. Tsunetsugu and M. Arikawa, J. Phys. Soc. Jpn. **75**, 083701 (2006).
[13] A. Laüchli, F. Mila, and K. Penc, Phys. Rev. Lett. **97**, 087205 (2006).
[14] S. Bhattacharjee, V. B. Shenoy, and T. Senthil, Phys. Rev. B **74**, 092406 (2006).
[15] E. M. Stoudenmire, S. Trebst, and L. Balents, Phys. Rev. B **79**, 214436 (2009).
[16] H. Kawamura and A. Yamamoto, J. Phys. Soc. Jpn. **76**, 073704 (2007).
[17] L. N. Bulaevskii, C. D. Batista, M. V. Mostovoy, and D. I. Khomskii, Phys. Rev. B **78**, 024402 (2008).
[18] S. Fujimoto, Phys. Rev. Lett. **103**, 047203 (2009).
[19] Y. Nambu *et al.*, J. Cryst. Growth **310**, 1881 (2008).
[20] A. Damascelli, Z. Hussain, and Z.-X. Shen, Rev. Mod. Phys. **75**, 473 (2003).
[21] I. I. Mazin, Phys. Rev. B **76**, 140406(R) (2007).
[22] K. Takubo, T. Mizokawa, Y. Nambu, and S. Nakatsuji, Phys. Rev. B **79**, 134422 (2009).
[23] Y. Qi and S. Sachdev, Phys. Rev. B **77**, 165112 (2008).
[24] N. F. Mott, *Metal-Insulator Transitions* (Taylor-Francis, London, 1974).
[25] B. I. Halperin and T. M. Rice, Rev. Mod. Phys. **40**, 755 (1968).